CERN-ACC-NOTE-2017-0033

23rd May 2017
rainer.wanzenberg@desy.de

Calculation of Wakefields and Higher Order Modes for the New Design of the Vacuum Chamber of the ALICE Experiment for the HL-LHC

R. Wanzenberg and O. Zagorodnova*
DESY, Notkestr. 85, 22603 Hamburg, Germany

Keywords: Wakefields, Higher Order Modes, ALICE vacuum chamber, HL-LHC

Summary

The High Luminosity Large Hadron Collider (HL-LHC) project was started with the goal to extend the discovery potential of the Large Hadron Collider (LHC). The HL-LHC study implies also upgraded dimensions of the ALICE beam pipe. The trapped monopole and dipole Higher Order Modes (HOMs) and the short range wakefields for the new design of the ALICE vacuum chamber were calculated with the help of the computer codes MAFIA and ECHO2D. The results of the short range wakefield calculations and the HOMs calculations for the ALICE vacuum chamber with new dimensions are presented in this report. The short range wakefields are presented in terms of longitudinal and transverse wake potentials and also in terms of loss and kick parameters. The frequency, the loss parameter, the R/Q and the Q-values and also power loss parameters are presented as result of the HOMs calculations and can be converted into impedance values.

The HL-LHC Design Study is included in the High Luminosity LHC project and is partly funded by the European Comission within the Framework Programme 7 Capacities Specific Programme, Grant Agreement 284404.

1 Introduction

1.1 The LHC accelerator

The High Luminosity LHC (HL-LHC) project was started in 2011 with the goal to extend the discovery potential of the LHC [1] by increasing the luminosity parameter by a factor 10 beyond its design value. The ALICE detector will be also upgraded with a new beam pipe. The results of the wakefield calculations and of the higher order modes calculations for the

*affiliated with DESY until 2015

ALICE vacuum chamber with new dimensions are presented in this report. A similar study was done for the CMS experiment [2] and for the ATLAS experiment [3].

Two options with different sets of parameters are considered for the HL-LHC. The parameters for both options are presented in the Table 1.

Parameter	Option 1	Option 2	
Beam energy	7	7	TeV
Ring circumference	26658.883	26658.883	m
Revolution frequency	11.245	11.245	kHz
RMS bunch length	7.5	7.5	cm
Number of bunches	2808	1404	
Number of particles per bunch	$2.2 \cdot 10^{11}$	$3.5 \cdot 10^{11}$	
Charge of one bunch	35.2	56.1	nC
Circulating beam current	1.11	0.89	A

Table 1: Two design parameters options for the HL-LHC.

A Gaussian bunch with an rms bunch length of 7.5 cm was used for the wake fields calculations. For the calculations of the power loss parameters the data from the Table 1 were used for both options of the HL-LHC.

1.2 The ALICE vacuum chamber

The ALICE vacuum chamber is installed in the ALICE (A Large Ion Collider Experiment) heavy-ion detector at the LHC ring. The ALICE beam pipe is about 38 m long and consists of round pipes and tapers with different radii, an elliptical pipe and two bellows. A schematic view of the IP region of the new ALICE beam pipe is shown in Fig. 1

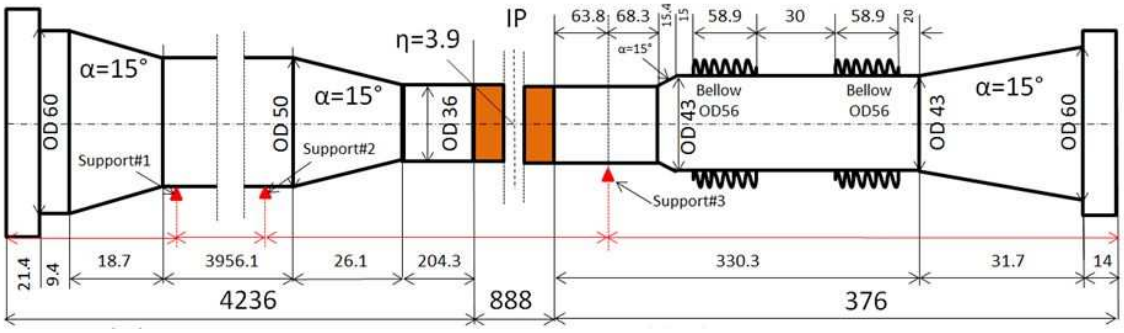

Figure 1: Schematic view of the IP region of the new ALICE beam pipe. All dimensions are in mm.

The cylindrically symmetric geometry was used for the calculations of the wakefields and higher order modes. A list of the r-z coordinates of the beam pipe is given in the Table 2. A plot of the r-z coordinates is shown in Fig. 2. This plot presents a two-dimensional model for the wakefield and HOMs calculations.

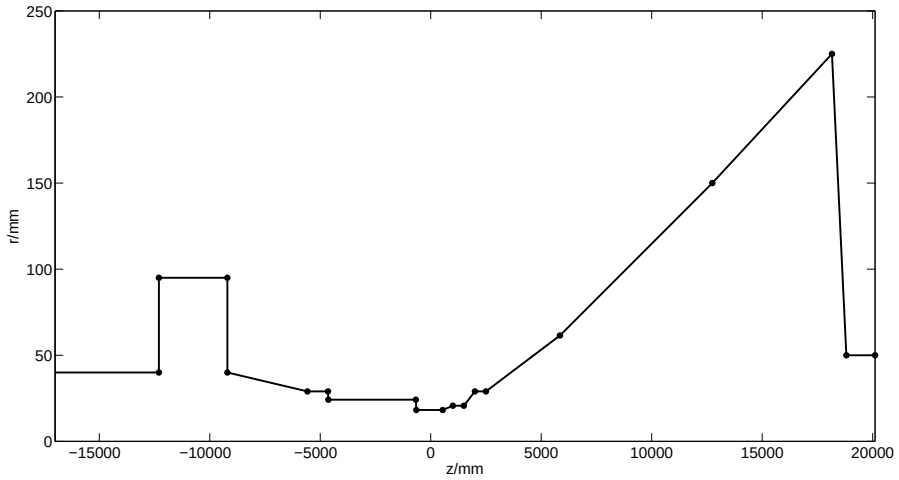

Figure 2: Schematic representation of the geometry of the ALICE structure. All dimensions are given in mm. The interaction point (IP) is at $z = 0$ mm.

	z/mm	r/mm	Comments
1	-18817	40.0	
2	-12300	40.0	
3	-12300	95.0	Elliptical cross section: 95 vertical, 67.5 horizontal
4	-9200	95.0	End of the elliptical cross section
5	-9200	40.0	
6	-5580	29.0	
7	-4649	29.0	
8	-4631	24.2	
9	-675	24.2	
10	-652	18.2	
11	0	18.2	IP
12	542	18.2	
13	551	20.7	
14	603	20.7	
15	603	20.7	Bellow Start
16	666	20.7	Bellow End
17	666	20.7	
18	694	20.7	
19	694	20.7	Bellow Start
20	757	20.7	Bellow End
21	757	20.7	
22	775	20.7	
23	806	29.0	
24	820	29.0	
25	5849	61.5	
26	12741	150.0	
27	18156	225.0	
28	18810	50.0	
29	19107	50.0	

Table 2: The main components of the ALICE beam pipe.

2 Wakefields

The ALICE beam pipe contains rotationally symmetric elements and a pipe with elliptical cross section. The elliptical pipe is 3.1 m long and has the following dimensions: r_{min}=67.5 mm, r_{max}=95 mm. For numerical wakefield calculations a two-dimensional (r, z) rotationally symmetric geometrical model with respect to the longitudinal axis was used (see Fig. 2). In this model a round pipe with a radius of 95 mm was used instead of the elliptical pipe. The monopole and dipole wakefields for this structure were calculated with help of two-dimensional computer code ECHO2D [4, 5].

Firstly, the geometry without bellows was used for the calculations. Then the wakefield of one bellow was calculated. And finally the geometry of the ALICE beam pipe with two bellows was investigated.

The ingoing pipe of the ALICE structure has a radius of 40 mm, and the outgoing pipe of this structure has a radius of 50 mm. Therefore the evaluation of the impact of the step-out transition on the result of the transverse wake potential was estimated.

2.1 Wake potentials

Numerical calculations with the help of the code ECHO2D give a possibility to obtain longitudinal monopole, longitudinal dipole and transverse dipole wake potentials. The wake potential [6] of a bunch with a charge q_1 is defined as:

$$\mathbf{W}(\mathbf{r}_{\perp 2}, \mathbf{r}_{\perp 1}, s) = \frac{1}{q_1} \int_0^L dz (\mathbf{E} + c\ \mathbf{e_z} \times \mathbf{B})_{t=(z+s)/c}. \tag{1}$$

In the case of cylindrically symmetric structure a multipole expansion can be used to describe the wake potential. Then, the longitudinal wake potential is given by the following formula:

$$W_{||}(r_1, r_2, \varphi_1, \varphi_2, s) = \sum_{m=0}^{\infty} r_1^m r_2^m W_{||}^{(m)}(s)\ \cos(m(\varphi_2 - \varphi_1)). \tag{2}$$

The functions $W_{||}^{(m)}(s)$ are the longitudinal m-pole wake potentials. The longitudinal and transverse components of the wake potential are connected by Panofsky-Wenzel theorem [7]. The transverse wake potential can be obtained by integration of the transverse gradient of the longitudinal wake potential:

$$W_{\perp}^{(m)}(s) = -\int_{-\infty}^{s} ds'\, W_{||}^{(m)}(s'). \tag{3}$$

The transverse dipole wake potential is given by:

$$W_{\perp}^{(1)}(s) = -\int_{-\infty}^{s} ds'\, W_{||}^{(0)}(s'). \tag{4}$$

2.2 Loss and Kick parameters

The numerical calculations provide the monopole and dipole wake potentials $W_{||}^{(0)}(s)$ and $W_{\perp}^{(1)}(s)$. The total loss and total kick parameters can be obtained with the help of the following formulas:

$$k_{||\mathrm{tot}}^{(0)} = \int ds\, W_{||}^{(0)}(s) g(s), \tag{5}$$

$$k_{\perp}^{(1)} = \int ds\, W_{\perp}^{(1)}(s) g(s), \tag{6}$$

where $g(s)$ is the normalized charge density of the bunch:

$$g(s) = \frac{1}{\sigma_z} \frac{1}{\sqrt{2\pi}} \exp\left(-\frac{1}{2} \left(\frac{s}{\sigma_z} \right)^2 \right). \tag{7}$$

A Gaussian bunch with an rms bunch length of $\sigma_z = 7.5$ cm was used for the numerical calculations of the wake potentials in the time domain.

The total kick parameter is related to the transverse impedance (see [8])

$$(Z_{\perp})_{eff} = 2\,\sqrt{\pi} \frac{\sigma_z}{c} k_{\perp}^{(1)}. \tag{8}$$

2.3 Wakefields of the ALICE vacuum chamber without bellows

The longitudinal monopole, the longitudinal dipole and the transverse dipole wake potentials, which are calculated with the code ECHO2D, are shown in Fig. 3, Fig. 4, and Fig. 5. The results for the loss and kick parameters are presented in Table 3.

The ingoing pipe of the ALICE beam pipe has a radius of 40 mm, and the outgoing pipe has a radius of 50 mm. Therefore the form of the transverse dipole wake potential depends on step-out effect (see Fig. 5).

Parameter	Results	Δz/cm	Δr/cm
$k_{\|\|\mathrm{tot}}^{(0)}$ (V/pC)	1.83E-02	0.1	0.05
$k_{\perp}^{(1)}$ (V/pCm)	4.81	0.1	0.05

Table 3: Results for the loss and kick parameters of the ALICE vacuum chamber for a Gaussian bunch with rms bunch length of $\sigma_z = 7.5$ cm.

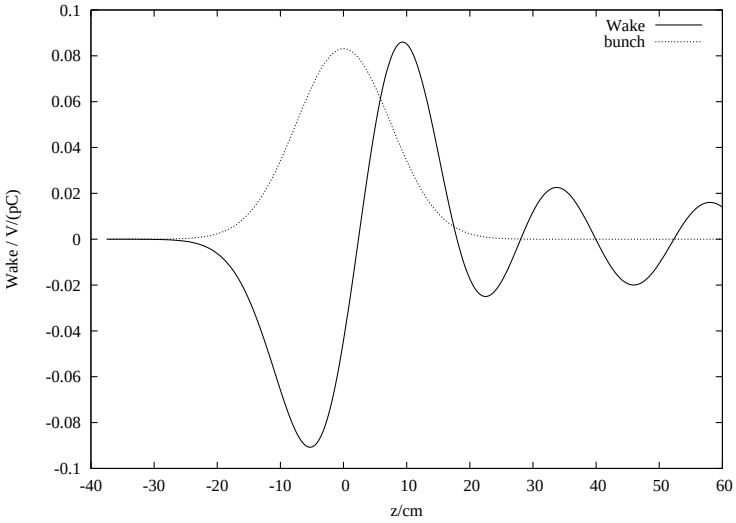

Figure 3: Longitudinal monopole wake potential of the ALICE vacuum chamber. The wake has been calculated with the ECHO2D code for an rms bunch length of 7.5 cm. Step sizes $\Delta z = 1$ mm in the longitudinal and $\Delta r = 0.5$ mm in the radial directions have been used for the calculations. The bunch shape is also shown (in arbitrary units).

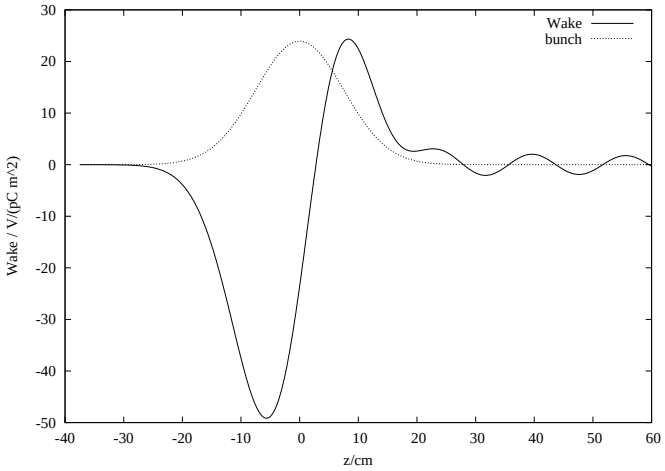

Figure 4: Longitudinal dipole wake potential of the ALICE vacuum chamber. The wake has been calculated with the ECHO2D code for an rms bunch length of 7.5 cm. Step sizes $\Delta z = 1$ mm in the longitudinal and $\Delta r = 0.5$ mm in the radial directions have been used for the calculations. The bunch shape is also shown (in arbitrary units).

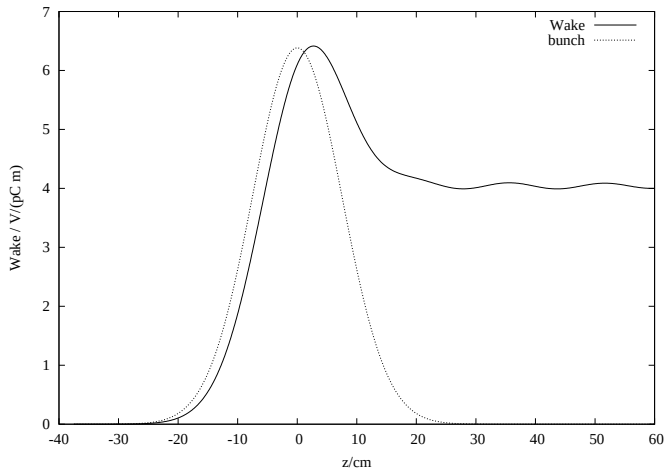

Figure 5: Transverse dipole wake potential of the ALICE vacuum chamber. The wake has been calculated with the ECHO2D code for an rms bunch length of 7.5 cm. Step sizes $\Delta z = 1$ mm in the longitudinal and $\Delta r = 0.5$ mm in the radial directions have been used for the calculations. The bunch shape is also shown (in arbitrary units).

2.4 Estimation of the step-out effect in the ALICE vacuum chamber

The form of the transverse dipole wake potential depends on the step-out transition between ingoing pipe ($r = 40$ mm) and outgoing pipe ($r = 50$ mm). In order to evaluate the impact of the step-out on the results, the transverse dipole wake potential of a step-out transition and transverse dipole wake potential of the ALICE structure with 40 mm outgoing pipe have been calculated. The comparison of the total kick parameters $k_{\perp}^{(1)}$ for the step-out transition from 40 mm to 50 mm, for the ALICE structure with different radii of the ingoing and outgoing beam pipes and for the ALICE structure with same radii of ingoing and outgoing pipes (40mm) are presented in Table 4. The kick parameter of the step-out transition gives a significant contribution to the total kick parameter of the whole structure.

Model	$k_{\perp}^{(1)}$ (V/pCm)
1) Step-out (from 40 mm to 50 mm)	2.18
2) ALICE structure with step-out	4.81
3) ALICE structure without step-out	2.88

Table 4: Results for the kick parameters of three different structures: 1) step-out transition, 2) ALICE structure with step-out,and 3) ALICE structure without step-out.

The transverse dipole wake potentials for these three structures are shown in Fig. 6.

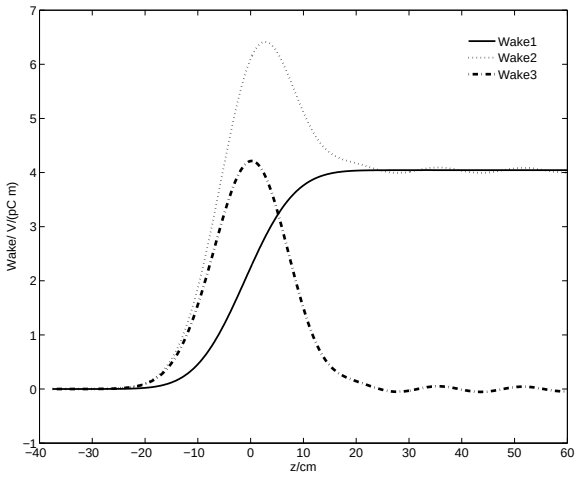

Figure 6: Comparison of the transverse dipole wake potentials for three different structures: 1) step-out transition, 2) ALICE structure with step-out, 3) ALICE structure without step-out. The wakes have been calculated with the ECHO2D code for an rms bunch length of 7.5 cm. Step sizes $\Delta z = 1$ mm in the longitudinal and $\Delta r = 0.5$ mm in the radial directions have been used for the calculation.

2.5 Wakefields of one bellow

There are two unshielded bellows with the same dimensions installed in the ALICE beam pipe. The positions of the bellows in the pipe are listed in Table 2. A view of the bellows with geometrical dimensions is shown in Fig. 7.

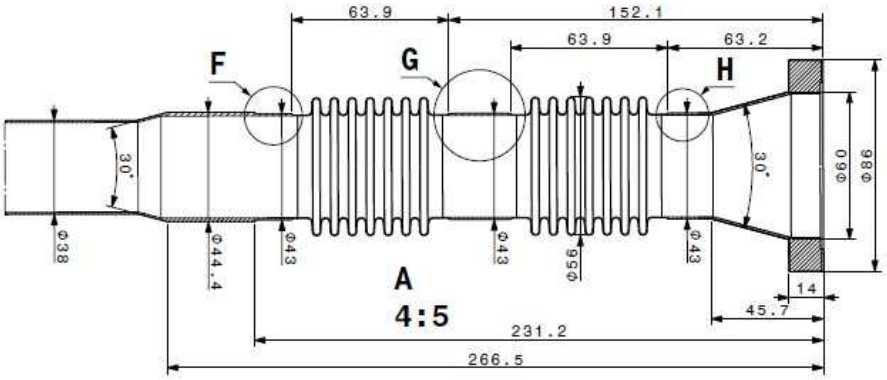

Figure 7: View of the bellows in the ALICE structure. The geometrical dimensions are in mm.

The results for the loss and kick parameters for one bellow are summarized in Table 5. The loss and the kick parameters are presented for two different step sizes of the mesh. The longitudinal monopole and the transverse dipole wake potentials, which are calculated with the ECHO2D code, are shown in Fig. 8, and Fig. 9. The transverse wake potential for

different mesh sizes is shown in Fig. 10.

Parameter	$\Delta z = 0.1$cm $\Delta r = 0.05$cm	$\Delta z = 0.2$cm $\Delta r = 0.1$cm
$k^{(0)}_{\|\|\mathrm{tot}}$ (V/pC)	≈ 0	≈ 0
$k^{(1)}_{\perp}$ (V/pCm)	2.0735	1.9361

Table 5: Results for the loss and kick parameters calculated for one bellow for a Gaussian bunch with rms bunch length of $\sigma_z = 7.5$ cm and two different step sizes of the mesh.

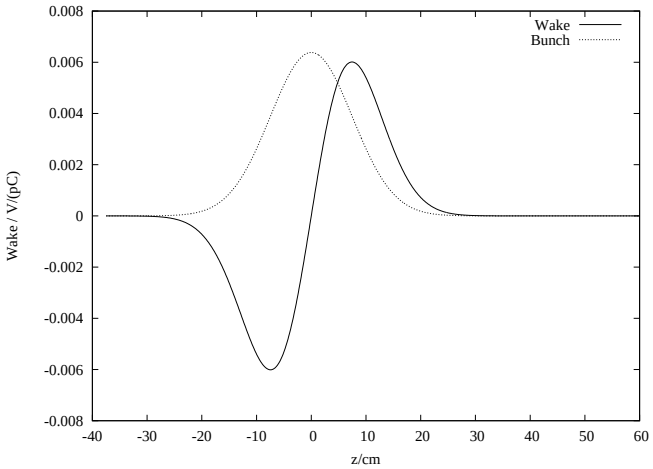

Figure 8: Longitudinal monopole wake potential of one bellow installed in the ALICE structure. The wake has been calculated with the ECHO2D code for an rms bunch length of 7.5 cm. Step sizes $\Delta z = 1$ mm in the longitudinal and $\Delta r = 0.5$ mm in the radial directions have been used for the calculation. The bunch shape is also shown (in arbitrary units).

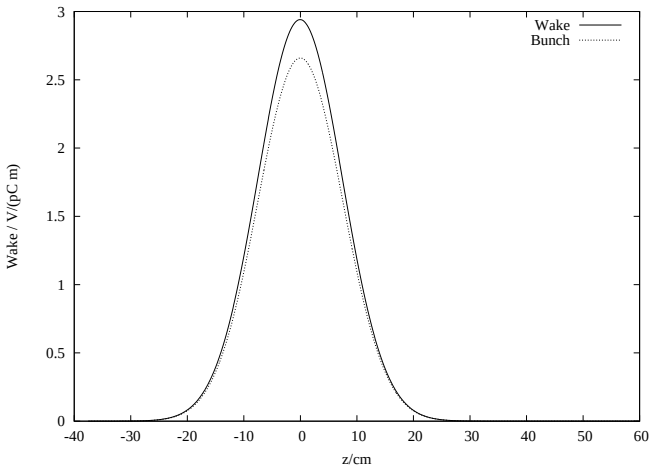

Figure 9: Transverse dipole wake potential of one bellow installed in the ALICE structure. The wake has been calculated with the ECHO2D code for an rms bunch length of 7.5 cm. Step sizes $\Delta z = 1$ mm in the longitudinal and $\Delta r = 0.5$ mm in the radial directions have been used for the calculation. The bunch shape is also shown (in arbitrary units).

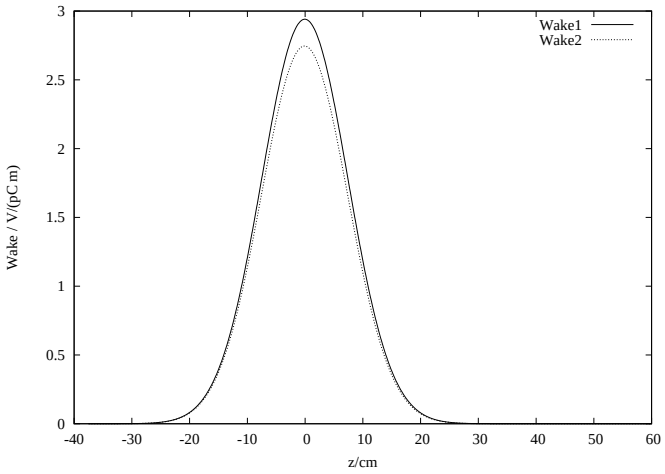

Figure 10: Comparison of the transverse dipole wake potentials of one bellow for different mesh size. For the calculation of the Wake1 step sizes $\Delta z = 1$ mm in the longitudinal and $\Delta r = 0.5$ mm in the radial directions have been used. For the calculation of the Wake2 the step sizes $\Delta z = 2$ mm and $\Delta r = 1$ mm have been used.

2.6 Wakefields of the ALICE chamber with bellows

The results of the wakefields calculations for one bellow were presented in the previous section. Now two bellows with the same geometrical dimensions are placed successively on one side of the IP (see Fig. 1). The distance between the bellows is about 3 cm. The plot of the transverse dipole wake potential is given in Fig. 11. The kick parameter $k_{\perp}^{(1)}$ for this structure is equal to 8.68 V/pCm. The results for the kick parameters for the ALICE

chamber without bellows, for one bellow and for the ALICE chamber with two bellows are presented in Table 6 for comparison.

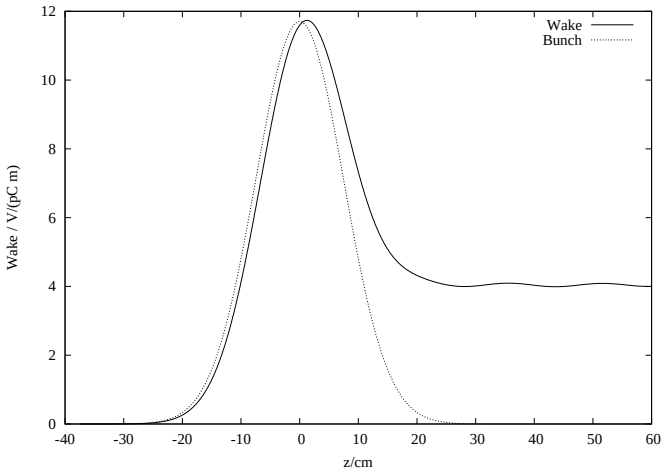

Figure 11: Transverse dipole wake potential of the ALICE structure and two bellows. Step sizes $\Delta z = 1$ mm in the longitudinal and $\Delta r = 0.5$ mm in the radial directions have been used for the calculation. The wake has been calculated for an rms bunch length of 7.5 cm. The bunch shape is also shown (in arbitrary units).

Type of structure	Kick parameter $k_{\perp}^{(1)}$(V/pCm)
ALICE chamber	
w/o bellows	4.81
One bellow	2.07
ALICE with two bellows	8.68

Table 6: Results for the kick parameters calculated for a Gaussian bunch with rms bunch length of $\sigma_z = 7.5$ cm, using a mesh with step sizes of $\Delta z = 1$ mm and $\Delta r = 0.5$ mm.

3 Higher Order Modes - HOMs

The electric and the magnetic fields of the higher order modes are calculated with the frequency domain solver of the computer code MAFIA [9, 10, 11]. A two-dimensional geometrical model (see Fig. 2) has been used to obtain all important rf-parameters. The round pipe with a radius of 95 mm was used in the region with elliptical cross section between 9.2 m to 12.3 m left from the IP.

The step sizes of the mesh of 1 mm in the radial (r) and 2 mm in the longitudinal (z) directions have been used for the calculations. Different sets of boundary conditions (electric (E) and magnetic (M)) were used at both ends of the modeled structure. A frequency estimation of 1.6 GHz was used for the calculation of 100 monopole, and of 2.0 GHz for the calculation of 100 dipole modes.The results of calculations are independent from the boundary conditions for all calculated monopole modes. The results for the dipole modes are independent from boundary conditions if a model with a longer (1.3 m) outgoing pipe is used.

All results are presented for electric (E) boundary conditions on both ends in Table 7, 8, 9 for monopole modes and in Table 13, 14, 15 for dipole modes. The modes are labeled as "EE-n" according to the boundary conditions and the mode number n, starting with the label "EE-1" for the mode with the lowest frequency.

3.1 The main parameters of frequency domain calculations

The eigenvalue solver of the code MAFIA provides the electric and the magnetic fields (E, B) of the higher order modes and the frequency ($f = \omega/(2\pi)$) for each mode on the mesh. Several parameters, including the stored energy U, voltage V, loss parameters $k_{||}(r)$, $k_{\perp}(r)/r^2$, R/Q, Q_{Cu}, Q_{Steel}, G_1, transverse impedance $Z_{\perp}$ and power loss P_{loss} were obtained as result of the post-processing [6].

The following relations are used in the post-processing for the frequency domain:

$$k_{||}(r) = \frac{\mid V(r) \mid^2}{4U}, \tag{9}$$

$$\frac{R}{Q} = \frac{2k_{||}(r)}{\omega}. \tag{10}$$

The Q-value is calculated from the field distribution on the wall of the vacuum chamber and the surface resistivity:

$$Q = \frac{\omega U}{P_{sur}}. \tag{11}$$

P_{sur} is the power dissipated into the cavity wall due to the surface resistivity R_{sur}. The dissipated power P_{sur} is calculated in the post-processor for a copper surface with resistivity:

$$R_{Cu} = \sqrt{\frac{\omega\mu_0}{2\sigma_{Cu}}},$$

$$\sigma_{Cu} = 5.8 \cdot 10^7 (\Omega m)^{-1}. \tag{12}$$

The Q-value of any material can be obtained by scaling the value for copper:

$$Q_{Mat} = \sqrt{\frac{\sigma_{Mat}}{\sigma_{Cu}}} Q_{Cu}, \tag{13}$$

where σ_{Mat} is the conductivity of the material. The conductivity of steel σ_{St} [12] is approximately equal to $1.5 \cdot 10^6 (\Omega m)^{-1}$

The parameter G_1 [13] is a purely geometric characteristic of the vacuum chamber:

$$G_1 = R_{Mat} Q_{Mat}. \tag{14}$$

The loss parameter $k_{||}(r)$ is calculated on axis of the chamber ($r = 0$) for monopole modes and at an offset of $r = 1$cm from the axis for dipole modes. Therefore, R/Q parameters for monopole and for dipole modes are defined as:

$$\frac{R^{(0)}}{Q} = \frac{2k_{||}(r=0)}{\omega}, \tag{15}$$

$$\frac{R^{(1)}}{Q} = \frac{1}{r^2} \frac{2k_{||}(r)}{\omega}. \tag{16}$$

The transverse impedance can be defined using the following relation:

$$Z_{\perp} = \frac{1}{\omega/c} \frac{R^1}{Q} Q_{Steel}. \tag{17}$$

The units of $R^{(0)}/Q$ are Ohm. The units of $R^{(1)}/Q$ and $Z_{\perp}$ are Ohm/m^2 and Ohm/m respectively.

The power loss parameters P_{loss} are obtained for two options of the HL-LHC (see Table 1) using the following relation:

$$P_{loss} = 2 \frac{R}{Q} Q_{Steel} I_{1,2}^2 e^{-(\frac{2\pi f_{hom}}{c})^2 \sigma_z^2}. \tag{18}$$

For the first option of the HL-LHC $I_1 = 1.11A$, for the second option $I_2 = 0.89A$. Parameters $R^{(0)}/Q$, $R^{(1)}/Q$ (see Eqs. (15), (16)) were used for the calculations of the power loss parameters for each monopole and each dipole mode.

The lists of the power loss parameters are presented in Table 10, 11, 12 for monopole modes and in Table 16, 17, 18 for dipole modes.

3.2 Monopole Modes

Calculations of 100 monopole modes were performed for different sets of boundary conditions on both ends of the ALICE beam pipe: ,,electric-electric", ,,electric-magnetic", ,,magnetic-magnetic". The results of calculations are independent from boundary conditions. Most of the higher order monopole modes are trapped in the regions with maximal radii of the beam pipe: from 9.2 m to 12.3 m left from the IP and from 10 m to 18.5 m right from the IP. The electric field of mode EE-1 ($f = 532.7$ MHz, $k^{(0)} = 0.21$ V/nC) is shown in Fig. 12, and the electric field of mode EE-87 ($f = 1303.6$ MHz, $k^{(0)} = 16.45$ V/nC) is shown in Fig. 13 in the

region between 16 m and 19 m right from the IP. The mode EE-87 is the mode with largest loss parameter.

The loss parameters of 100 monopole modes are plotted versus the mode frequency in Fig. 14.

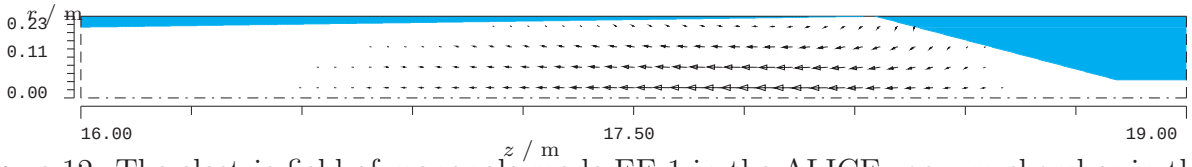

Figure 12: The electric field of monopole mode EE-1 in the ALICE vacuum chamber in the region between 16 m and 19 m.

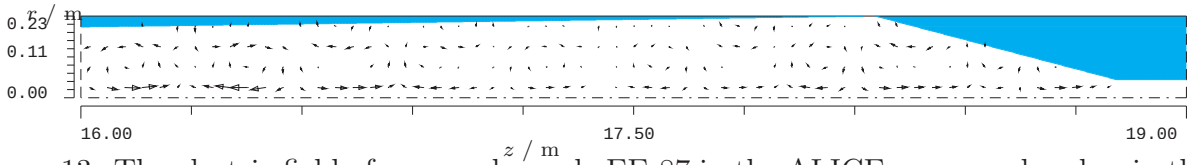

Figure 13: The electric field of monopole mode EE-87 in the ALICE vacuum chamber in the region between 16 m and 19 m.

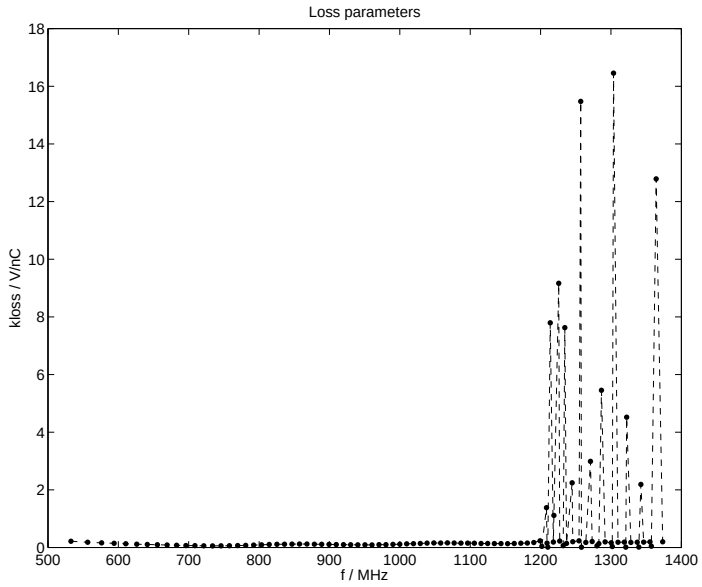

Figure 14: Plot of the loss parameters of the monopole modes versus frequency using the data from Tables 7, 8 and 9. The data points are marked (the dotted line is intended only to guide the eye).

Mode	f/MHz	$k^{(0)}$ (V/nC)	G_1 (Ohm)	R/Q (Ohm)	Q_{Cu}	Q_{Steel}
EE-1	532.7	0.2146	452.7	0.1282	75173	12089
EE-2	556.4	0.1816	460.3	0.1039	74790	12027
EE-3	576.2	0.1592	466.5	0.0879	74485	11978
EE-4	594.1	0.1443	472.0	0.0773	74225	11936
EE-5	610.6	0.1288	477.0	0.0672	73993	11899
EE-6	626.2	0.1144	481.8	0.0581	73792	11866
EE-7	641.1	0.1042	486.2	0.0518	73606	11837
EE-8	655.5	0.0931	490.5	0.0452	73437	11809
EE-9	669.4	0.0842	494.6	0.0400	73279	11784
EE-10	682.9	0.0759	498.6	0.0354	73127	11760
EE-11	696.0	0.0668	502.4	0.0305	72986	11737
EE-12	708.9	0.0640	506.3	0.0287	72881	11720
EE-13	721.5	0.0586	509.7	0.0259	72737	11697
EE-14	733.8	0.0558	513.3	0.0242	72621	11678
EE-15	745.9	0.0569	516.6	0.0243	72499	11659
EE-16	757.9	0.0606	519.6	0.0254	72347	11634
EE-17	769.6	0.0652	522.7	0.0269	72226	11615
EE-18	781.1	0.0731	525.0	0.0298	72002	11579
EE-19	792.3	0.0825	527.5	0.0331	71832	11551
EE-20	803.4	0.0921	529.9	0.0365	71657	11523
EE-21	814.4	0.1038	532.9	0.0406	71580	11511
EE-22	825.3	0.1105	535.6	0.0426	71456	11491
EE-23	836.1	0.1142	537.9	0.0435	71309	11467
EE-24	846.8	0.1177	541.0	0.0443	71255	11459
EE-25	857.4	0.1182	543.6	0.0439	71150	11442
EE-26	868.0	0.1179	546.3	0.0432	71068	11428
EE-27	878.5	0.1144	549.1	0.0414	71013	11420
EE-28	889.0	0.1109	551.8	0.0397	70937	11407
EE-29	899.4	0.1058	554.9	0.0374	70916	11404
EE-30	909.7	0.1005	557.2	0.0352	70812	11387
EE-31	920.0	0.0980	560.3	0.0339	70801	11385
EE-32	930.2	0.0935	562.7	0.0320	70718	11372
EE-33	940.3	0.0915	565.5	0.0310	70691	11368

Table 7: Monopole modes of the ALICE vacuum chamber.

Mode	f/MHz	$k^{(0)}$ (V/nC)	G_1 (Ohm)	R/Q (Ohm)	Q_{Cu}	Q_{Steel}
EE-34	950.4	0.0923	568.3	0.0309	70657	11362
EE-35	960.4	0.0893	570.7	0.0296	70586	11351
EE-36	970.4	0.0968	573.4	0.0317	70558	11346
EE-37	980.3	0.0962	575.8	0.0312	70490	11335
EE-38	990.1	0.1083	578.1	0.0348	70422	11325
EE-39	999.9	0.1143	580.4	0.0364	70357	11314
EE-40	1009.7	0.1269	583.4	0.0400	70372	11317
EE-41	1019.4	0.1328	585.1	0.0415	70237	11295
EE-42	1029.1	0.1392	587.4	0.0431	70179	11285
EE-43	1038.7	0.1517	590.3	0.0465	70201	11289
EE-44	1048.4	0.1551	592.5	0.0471	70139	11279
EE-45	1058.0	0.1549	594.8	0.0466	70089	11271
EE-46	1067.6	0.1592	597.4	0.0475	70082	11270
EE-47	1077.2	0.1542	599.4	0.0456	70004	11257
EE-48	1086.8	0.1519	602.7	0.0445	70076	11269
EE-49	1096.3	0.1500	604.2	0.0436	69948	11248
EE-50	1105.9	0.1477	607.5	0.0425	70018	11260
EE-51	1115.4	0.1383	608.8	0.0395	69872	11236
EE-52	1124.9	0.1376	613.1	0.0389	70070	11268
EE-53	1134.4	0.1335	614.1	0.0375	69886	11238
EE-54	1143.8	0.1334	617.1	0.0371	69937	11247
EE-55	1153.2	0.1313	619.5	0.0362	69924	11244
EE-56	1162.6	0.1376	621.6	0.0377	69878	11237
EE-57	1171.9	0.1458	624.6	0.0396	69937	11247
EE-58	1181.2	0.1529	626.0	0.0412	69819	11228
EE-59	1190.4	0.1713	629.9	0.0458	69973	11252
EE-60	1199.2	0.2296	679.6	0.0609	75216	12096
EE-61	1201.9	0.0391	907.3	0.0104	100317	16132
EE-62	1208.4	1.3805	446.3	0.3637	49206	7913
EE-63	1209.1	0.1506	639.0	0.0396	70439	11327
EE-64	1210.3	0.0115	441.8	0.0030	48676	7827
EE-65	1213.8	7.7933	437.7	2.0438	48156	7744
EE-66	1218.2	0.1871	638.6	0.0489	70135	11278

Table 8: Monopole modes of the ALICE vacuum chamber.

Mode	f/MHz	$k^{(0)}$ (V/nC)	G_1 (Ohm)	R/Q (Ohm)	Q_{Cu}	Q_{Steel}
EE-67	1218.9	1.1131	435.4	0.2907	47797	7686
EE-68	1225.8	9.1636	434.9	2.3796	47610	7656
EE-69	1227.2	0.2219	651.4	0.0576	71273	11461
EE-70	1232.2	0.0635	963.0	0.0164	105156	16910
EE-71	1234.4	7.6275	436.0	1.9668	47560	7648
EE-72	1236.9	0.1410	656.8	0.0363	71584	11511
EE-73	1244.9	2.2429	438.3	0.5735	47612	7656
EE-74	1245.8	0.2007	646.4	0.0513	70194	11288
EE-75	1254.6	0.2296	675.4	0.0583	73085	11753
EE-76	1257.0	15.4751	441.6	3.9186	47740	7677
EE-77	1258.0	0.0069	958.9	0.0017	103629	16665
EE-78	1264.3	0.1742	654.4	0.0439	70540	11344
EE-79	1270.9	2.9886	445.8	0.7485	47928	7707
EE-80	1273.3	0.2059	654.9	0.0515	70352	11313
EE-81	1280.2	0.0589	966.7	0.0146	103557	16653
EE-82	1282.9	0.1328	686.1	0.0329	73427	11808
EE-83	1286.5	5.4528	450.7	1.3492	48166	7745
EE-84	1291.7	0.1923	656.7	0.0474	70034	11262
EE-85	1300.3	0.1641	756.1	0.0402	80374	12925
EE-86	1301.8	0.0340	872.3	0.0083	92668	14902
EE-87	1303.6	16.4530	456.3	4.0173	48444	7790
EE-88	1310.0	0.1803	660.3	0.0438	69924	11244
EE-89	1319.0	0.1834	680.5	0.0443	71817	11549
EE-90	1321.1	0.0110	1023.1	0.0026	107891	17350
EE-91	1322.3	4.5191	462.6	1.0878	48759	7841
EE-92	1328.2	0.1765	663.3	0.0423	69758	11218
EE-93	1337.3	0.1818	671.9	0.0433	70430	11326
EE-94	1339.5	0.0151	1059.8	0.0036	110988	17848
EE-95	1342.5	2.1890	469.4	0.5190	49103	7896
EE-96	1346.4	0.1855	667.8	0.0439	69757	11218
EE-97	1355.5	0.1952	669.1	0.0458	69655	11201
EE-98	1357.4	0.0434	1079.7	0.0102	112329	18064
EE-99	1364.2	12.7864	514.5	2.9835	53392	8586
EE-100	1373.6	0.1974	659.6	0.0457	68215	10970

Table 9: Monopole modes of the ALICE vacuum chamber.

Mode	f/MHz	$P_{loss}(W)$ Option 1	$P_{loss}(W)$ Option 2
EE-1	532.7	1904.5	1204.1
EE-2	556.4	1440.3	910.7
EE-3	576.2	1148.7	726.3
EE-4	594.1	956.0	604.4
EE-5	610.6	788.1	498.3
EE-6	626.2	648.7	410.1
EE-7	641.1	549.7	347.6
EE-8	655.5	457.4	289.2
EE-9	669.4	386.3	244.3
EE-10	682.9	325.7	205.9
EE-11	696.0	268.2	169.6
EE-12	708.9	240.9	152.3
EE-13	721.5	207.1	130.9
EE-14	733.8	185.1	117.0
EE-15	745.9	177.5	112.2
EE-16	757.9	177.4	112.1
EE-17	769.6	179.5	113.5
EE-18	781.1	189.3	119.7
EE-19	792.3	201.0	127.1
EE-20	803.4	211.3	133.6
EE-21	814.4	224.7	142.1
EE-22	825.3	225.4	142.5
EE-23	836.1	219.6	138.9
EE-24	846.8	213.7	135.1
EE-25	857.4	202.3	127.9
EE-26	868.0	190.2	120.3
EE-27	878.5	174.1	110.1
EE-28	889.0	159.3	100.7
EE-29	899.4	143.4	90.6
EE-30	909.7	128.4	81.2
EE-31	920.0	118.2	74.7
EE-32	930.2	106.3	67.2
EE-33	940.3	98.1	62.0

Table 10: Power loss parameters for the monopole modes of the ALICE vacuum chamber for two options of the HL-LHC.

Mode	f/MHz	$P_{loss}(W)$ Option 1	$P_{loss}(W)$ Option 2
EE-34	950.4	93.4	59.0
EE-35	960.4	85.2	53.9
EE-36	970.4	87.1	55.1
EE-37	980.3	81.7	51.6
EE-38	990.1	86.7	54.8
EE-39	999.9	86.2	54.5
EE-40	1009.7	90.4	57.1
EE-41	1019.4	89.0	56.3
EE-42	1029.1	87.9	55.6
EE-43	1038.7	90.4	57.1
EE-44	1048.4	87.0	55.0
EE-45	1058.0	81.9	51.8
EE-46	1067.6	79.3	50.1
EE-47	1077.2	72.2	45.7
EE-48	1086.8	67.1	42.4
EE-49	1096.3	62.3	39.4
EE-50	1105.9	57.8	36.5
EE-51	1115.4	50.8	32.1
EE-52	1124.9	47.7	30.1
EE-53	1134.4	43.4	27.4
EE-54	1143.8	40.8	25.8
EE-55	1153.2	37.8	23.9
EE-56	1162.6	37.2	23.5
EE-57	1171.9	37.1	23.4
EE-58	1181.2	36.5	23.1
EE-59	1190.4	38.5	24.4
EE-60	1199.2	52.3	33.1
EE-61	1201.9	11.7	7.4
EE-62	1208.4	193.3	122.2
EE-63	1209.1	30.0	19.0
EE-64	1210.3	1.6	1.0
EE-65	1213.8	1029.2	650.7
EE-66	1218.2	34.9	22.1

Table 11: Power loss parameters for the monopole modes of the ALICE vacuum chamber for two options of the HL-LHC.

Mode	f/MHz	$P_{loss}(W)$ Option 1	$P_{loss}(W)$ Option 2
EE-67	1218.9	140.9	89.1
EE-68	1225.8	1102.2	696.9
EE-69	1227.2	39.6	25.0
EE-70	1232.2	16.1	10.2
EE-71	1234.4	863.4	545.9
EE-72	1236.9	23.6	14.9
EE-73	1244.9	236.4	149.5
EE-74	1245.8	31.0	19.6
EE-75	1254.6	34.7	21.9
EE-76	1257.0	1502.3	949.8
EE-77	1258.0	1.4	0.9
EE-78	1264.3	23.7	15.0
EE-79	1270.9	264.1	167.0
EE-80	1273.3	26.3	16.6
EE-81	1280.2	10.5	6.7
EE-82	1282.9	16.5	10.4
EE-83	1286.5	433.6	274.2
EE-84	1291.7	21.4	13.5
EE-85	1300.3	19.7	12.5
EE-86	1301.8	4.7	2.9
EE-87	1303.6	1163.7	735.8
EE-88	1310.0	17.6	11.1
EE-89	1319.0	17.2	10.9
EE-90	1321.1	1.5	1.0
EE-91	1322.3	281.0	177.6
EE-92	1328.2	15.0	9.5
EE-93	1337.3	14.6	9.3
EE-94	1339.5	1.9	1.2
EE-95	1342.5	118.2	74.7
EE-96	1346.4	13.8	8.7
EE-97	1355.5	13.6	8.6
EE-98	1357.4	4.8	3.0
EE-99	1364.2	639.0	404.0
EE-100	1373.6	11.7	7.4

Table 12: Power loss parameters for the monopole modes of the ALICE vacuum chamber for two options of the HL-LHC.

The longitudinal impedance due to HOMs can be obtained with the help of the following relation:

$$Z_{||}(\omega) = \sum_n \frac{R_n^{(0)}}{1 - i\,Q_n(\omega/\omega_n - \omega_n/\omega)}, \tag{19}$$

where

$$R_n^{(0)} = Q_{Steel,n} \left(\frac{R^{(0)}}{Q}\right)_n \tag{20}$$

is the shunt impedance of mode n using the Q-value of mode n for steel. The real part of the longitudinal impedance is plotted in Fig. 15.

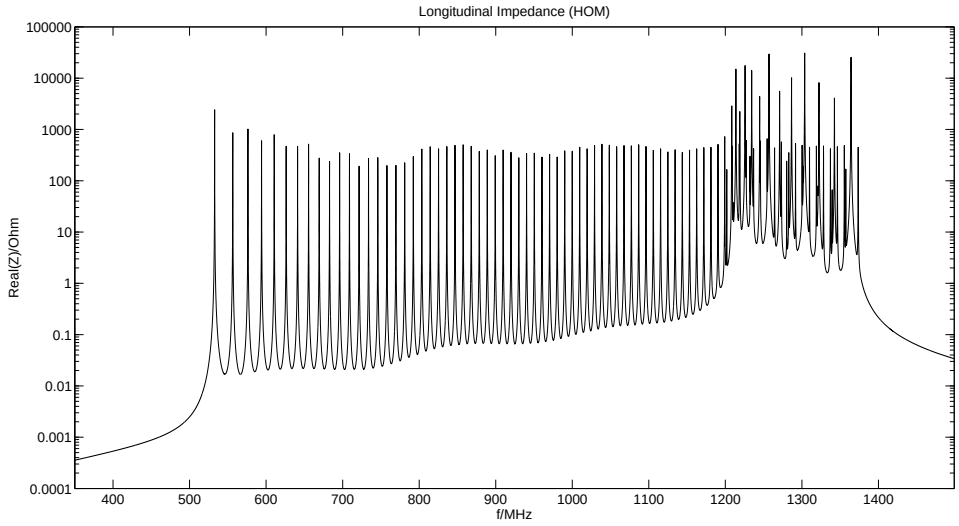

Figure 15: Real part of the longitudinal impedance due to HOMs using the data from Tables 7, 8 and 9.

3.3 Dipole Modes

Calculations of 100 dipole modes, as well as calculations of the monopole modes, were performed for different sets of boundary conditions: ,,electric-electric", ,,electric-magnetic", ,,magnetic-magnetic". The results of the calculations for dipole modes were dependent on boundary conditions. The length of the outgoing pipe of the ALICE structure is about 0.3 m. A small length of the outgoing pipe did not allow to obtain results independent from the boundary conditions for dipole modes. In order to obtain such results the outgoing pipe with the length of 1.3 m was used. All results for the dipole modes are given for longer (1.3 m) outgoing pipe. The electric field of mode EE-1 ($f = 413.8$ MHz, $k^{(1)}(r)/r^2 = 2.92$ V/(nCm^2)) is shown in Fig. 16, and the electric field of mode EE-96 ($f = 1116.1$ MHz, $k^{(1)}(r)/r^2 = 75.24$ V/(nCm^2)) is shown in Fig. 17 in the region between 16 m and 19 m right from the IP.

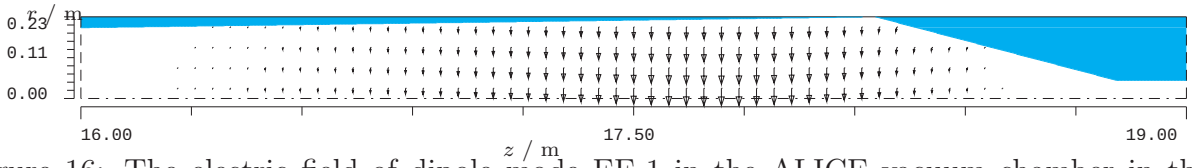

Figure 16: The electric field of dipole mode EE-1 in the ALICE vacuum chamber in the region between 16 m and 19 m right from the IP.

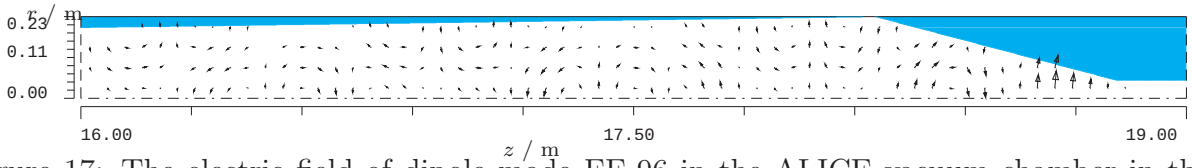

Figure 17: The electric field of dipole mode EE-96 in the ALICE vacuum chamber in the region between 16 m and 19 m right from the IP.

Mode	f/MHz	$k^{(1)}(r)/r^2$ /$(V/(nCm^2))$	G_1 (Ohm)	Q_{Cu}	Q_{Steel}	$Z_\perp$ /Ohm/m
EE-1	413.8	2.92	259.7	48933	7869	2041.06
EE-2	435.4	3.14	270.4	49678	7989	2008.86
EE-3	453.5	3.26	279.3	50273	8084	1944.04
EE-4	469.9	3.34	287.3	50799	8169	1876.37
EE-5	485.1	3.35	294.6	51263	8243	1782.04
EE-6	499.5	3.32	301.4	51691	8312	1679.96
EE-7	513.3	3.22	307.9	52094	8377	1555.75
EE-8	526.6	3.10	314.2	52476	8439	1430.91
EE-9	539.5	2.92	320.1	52825	8495	1292.61
EE-10	552.0	2.71	325.9	53158	8548	1153.87
EE-11	564.3	2.48	331.5	53483	8600	1018.28
EE-12	576.3	2.26	336.8	53772	8647	892.40
EE-13	588.1	2.06	341.8	54015	8686	784.07
EE-14	599.7	1.93	346.0	54164	8710	709.17
EE-15	611.0	1.79	350.0	54280	8729	636.43
EE-16	622.1	1.74	354.6	54491	8763	597.24
EE-17	633.0	1.77	359.6	54782	8809	591.55
EE-18	643.8	1.83	364.0	54979	8841	594.12
EE-19	654.5	2.00	368.3	55174	8872	629.78
EE-20	665.1	2.23	373.1	55454	8917	683.38
EE-21	675.6	2.46	377.7	55690	8955	732.12
EE-22	686.0	2.72	382.0	55898	8989	789.97
EE-23	696.3	3.02	386.2	56098	9021	852.47
EE-24	706.5	3.25	390.6	56322	9057	895.22
EE-25	716.7	3.45	395.2	56579	9098	928.69
EE-26	726.8	3.57	399.3	56775	9130	935.88
EE-27	736.8	3.64	403.4	56960	9160	934.08
EE-28	746.7	3.72	407.4	57139	9188	931.06
EE-29	756.6	3.72	411.6	57357	9223	911.02
EE-30	766.4	3.68	416.0	57602	9263	880.28
EE-31	776.2	3.46	420.0	57773	9290	809.31
EE-32	786.0	3.33	423.7	57934	9316	761.60
EE-33	795.6	3.03	427.6	58105	9344	678.27

Table 13: Dipole modes of the ALICE vacuum chamber.

Mode	f/MHz	$k^{(1)}(r)/r^2$ $/(V/(nCm^2))$	G_1 (Ohm)	Q_{Cu}	Q_{Steel}	$Z_\perp$ /Ohm/m
EE-34	805.3	2.80	431.5	58280	9372	615.67
EE-35	814.9	2.60	435.8	58516	9410	559.87
EE-36	824.4	2.21	440.3	58775	9452	465.83
EE-37	833.9	1.49	447.6	59418	9555	310.38
EE-38	839.7	4.41	686.7	90829	14606	1388.84
EE-39	843.8	4.28	456.7	60263	9691	885.62
EE-40	853.1	2.81	452.5	59386	9550	560.73
EE-41	862.5	2.13	458.7	59867	9627	418.02
EE-42	867.1	5.14	713.6	92889	14938	1549.46
EE-43	872.1	3.92	461.9	59951	9641	755.57
EE-44	881.4	3.29	463.8	59875	9628	619.56
EE-45	889.7	2.71	695.3	89344	14368	745.99
EE-46	890.9	5.80	484.7	62238	10008	1110.80
EE-47	900.2	4.03	471.3	60216	9683	731.19
EE-48	909.5	2.79	489.0	62148	9994	511.79
EE-49	910.1	5.45	711.1	90350	14529	1452.43
EE-50	918.8	4.42	478.8	60538	9735	774.73
EE-51	926.0	0.38	245.3	30896	4968	33.33
EE-52	928.1	4.62	482.0	60644	9752	793.61
EE-53	928.8	3.34	748.6	94152	15141	889.43
EE-54	929.7	0.00	247.6	31124	5005	0.03
EE-55	936.0	3.39	251.4	31503	5066	297.75
EE-56	937.4	4.75	485.5	60785	9775	802.59
EE-57	944.6	1.24	256.8	32030	5150	108.67
EE-58	946.4	4.57	641.9	79973	12861	996.34
EE-59	946.7	2.90	551.8	68737	11054	543.29
EE-60	955.6	4.70	263.7	32702	5259	410.95
EE-61	955.8	4.88	493.5	61186	9839	797.86
EE-62	963.3	2.32	746.3	92171	14822	562.01
EE-63	965.1	4.51	502.2	61964	9964	732.97
EE-64	968.9	12.94	272.2	33517	5390	1128.44
EE-65	974.2	4.86	501.6	61602	9906	770.93
EE-66	979.5	1.56	757.8	92808	14925	369.60

Table 14: Dipole modes of the ALICE vacuum chamber.

Mode	f/MHz	$k^{(1)}(r)/r^2$ $/(V/(nCm^2))$	G_1 (Ohm)	Q_{Cu}	Q_{Steel}	$Z_\perp$ /Ohm/m
EE-67	983.4	4.87	506.9	61963	9964	761.67
EE-68	984.3	0.52	282.1	34468	5543	44.85
EE-69	992.4	4.68	512.3	62329	10023	723.77
EE-70	995.1	1.30	758.1	92110	14812	296.44
EE-71	1001.6	4.83	513.3	62162	9996	731.30
EE-72	1001.9	15.02	293.6	35553	5717	1298.96
EE-73	1010.0	1.36	685.2	82645	13290	268.43
EE-74	1011.0	4.46	562.6	67827	10907	722.83
EE-75	1019.8	4.77	520.1	62428	10039	699.07
EE-76	1021.4	32.80	306.5	36763	5912	2822.81
EE-77	1024.9	0.82	769.7	92160	14820	176.15
EE-78	1028.9	4.81	525.1	62751	10091	696.42
EE-79	1037.8	3.93	540.3	64285	10338	572.30
EE-80	1039.4	1.51	750.9	89270	14356	305.62
EE-81	1042.7	8.59	320.9	38094	6126	734.64
EE-82	1047.0	4.87	530.4	62833	10104	682.07
EE-83	1053.2	0.48	774.8	91512	14716	97.56
EE-84	1056.1	5.23	537.3	63375	10191	725.51
EE-85	1065.0	4.81	542.8	63754	10252	659.76
EE-86	1065.8	6.85	336.9	39557	6361	582.16
EE-87	1067.3	0.20	775.0	90933	14623	39.64
EE-88	1074.1	5.36	542.0	63390	10194	719.25
EE-89	1080.4	0.45	785.2	91569	14725	86.19
EE-90	1083.1	5.92	552.5	64347	10348	793.68
EE-91	1090.6	55.07	355.4	41245	6632	4663.90
EE-92	1093.7	0.74	797.1	92383	14856	139.82
EE-93	1101.0	6.01	557.3	64377	10352	779.82
EE-94	1106.6	1.34	796.4	91765	14757	245.73
EE-95	1110.0	6.77	556.3	63996	10291	859.07
EE-96	1116.1	75.24	433.1	49694	7991	7330.18
EE-97	1117.4	54.63	434.1	49773	8004	5318.81
EE-98	1119.6	4.92	718.6	82321	13238	788.46
EE-99	1131.9	1.02	810.6	92354	14852	179.30
EE-100	1133.6	48.13	813.3	92587	14889	8469.89

Table 15: Dipole modes of the ALICE vacuum chamber.

Mode	f/MHz	$P_{loss}/r^2/(W/m^2)$ Option 1	$P_{loss}/r^2/(W/m^2)$ Option 2
EE-1	413.8	18162.5	28726.4
EE-2	435.4	17975.8	28431.0
EE-3	453.5	17412.8	27540.5
EE-4	469.9	16775.1	26531.9
EE-5	485.1	15867.6	25096.6
EE-6	499.5	14872.5	23522.8
EE-7	513.3	13673.1	21625.7
EE-8	526.6	12468.3	19720.3
EE-9	539.5	11153.6	17640.8
EE-10	552.0	9849.0	15577.4
EE-11	564.3	8589.1	13584.7
EE-12	576.3	7431.5	11753.9
EE-13	588.1	6440.7	10186.8
EE-14	599.7	5741.9	9081.5
EE-15	611.0	5075.6	8027.7
EE-16	622.1	4688.4	7415.3
EE-17	633.0	4567.7	7224.4
EE-18	643.8	4509.3	7132.0
EE-19	654.5	4695.5	7426.5
EE-20	665.1	5001.9	7911.1
EE-21	675.6	5257.1	8314.8
EE-22	686.0	5561.9	8796.8
EE-23	696.3	5881.3	9302.1
EE-24	706.5	6048.8	9567.0
EE-25	716.7	6141.9	9714.2
EE-26	726.8	6054.8	9576.4
EE-27	736.8	5908.5	9345.1
EE-28	746.7	5755.4	9102.8
EE-29	756.6	5500.4	8699.6
EE-30	766.4	5188.3	8206.0
EE-31	776.2	4654.0	7360.9
EE-32	786.0	4271.1	6755.3
EE-33	795.6	3707.7	5864.2

Table 16: Power loss parameters for the dipole modes of the ALICE vacuum chamber for two options of the HL-LHC.

Mode	f/MHz	$P_{loss}/r^2/(W/m^2)$ Option 1	$P_{loss}/r^2/(W/m^2)$ Option 2
EE-34	805.3	3278.9	5186.0
EE-35	814.9	2903.6	4592.3
EE-36	824.4	2351.4	3719.0
EE-37	833.9	1524.4	2411.1
EE-38	839.7	6704.8	10604.4
EE-39	843.8	4224.8	6682.0
EE-40	853.1	2600.7	4113.3
EE-41	862.5	1883.7	2979.3
EE-42	867.1	6881.6	10884.1
EE-43	872.1	3304.1	5225.8
EE-44	881.4	2629.7	4159.1
EE-45	889.7	3082.5	4875.4
EE-46	890.9	4570.9	4229.5
EE-47	900.2	2918.3	4615.6
EE-48	909.5	1979.7	3131.2
EE-49	910.1	5605.6	8866.0
EE-50	918.8	2902.2	4590.2
EE-51	926.0	121.8	192.6
EE-52	928.1	2878.4	4552.5
EE-53	928.8	3218.0	5089.8
EE-54	929.7	0.1	0.2
EE-55	936.0	1050.4	1661.4
EE-56	937.4	2817.2	4455.8
EE-57	944.6	371.7	587.8
EE-58	946.4	3386.2	5355.6
EE-59	946.7	1844.1	2916.6
EE-60	955.6	1350.3	2135.7
EE-61	955.8	2619.7	4143.4
EE-62	963.3	1795.2	2839.3
EE-63	965.1	2325.6	3678.3
EE-64	968.9	3529.5	5582.4
EE-65	974.2	2363.7	3738.4
EE-66	979.5	1110.6	1756.6

Table 17: Power loss parameters for the dipole modes of the ALICE vacuum chamber for two options of the HL-LHC.

Mode	f/MHz	$P_{loss}/r^2/(W/m^2)$ Option 1	$P_{loss}/r^2/(W/m^2)$ Option 2
EE-67	983.4	2254.7	3566.1
EE-68	984.3	132.3	209.2
EE-69	992.4	2068.7	3271.9
EE-70	995.1	838.4	1326.1
EE-71	1001.6	2016.1	3188.8
EE-72	1001.9	3577.9	5658.8
EE-73	1010.0	715.9	1132.3
EE-74	1011.0	1920.1	3036.8
EE-75	1019.8	1792.0	2834.3
EE-76	1021.4	7190.2	11372.2
EE-77	1024.9	442.3	699.5
EE-78	1028.9	1719.9	2720.2
EE-79	1037.8	1362.2	2154.5
EE-80	1039.4	722.8	1143.2
EE-81	1042.7	1713.2	2709.6
EE-82	1047.0	1562.3	2470.9
EE-83	1053.2	217.6	344.2
EE-84	1056.1	1598.8	2528.8
EE-85	1065.0	1399.4	2213.4
EE-86	1065.8	1230.3	1945.8
EE-87	1067.3	83.2	131.7
EE-88	1074.1	1466.5	2319.4
EE-89	1080.4	170.9	270.3
EE-90	1083.1	1555.0	2459.4
EE-91	1090.6	8838.8	13979.7
EE-92	1093.7	261.3	413.3
EE-93	1101.0	1409.9	2230.0
EE-94	1106.6	433.3	685.2
EE-95	1110.0	1490.8	2357.9
EE-96	1116.1	12368.6	19562.6
EE-97	1117.4	8924.1	14114.5
EE-98	1119.6	1309.1	2070.5
EE-99	1131.9	281.1	444.7
EE-100	1133.6	13171.5	20832.5

Table 18: Power loss parameters for the dipole modes of the ALICE vacuum chamber for two options of the HL-LHC.

The loss parameters of 100 dipole modes at a radius $r = 1$ cm are plotted versus the mode frequency in Fig. 18.

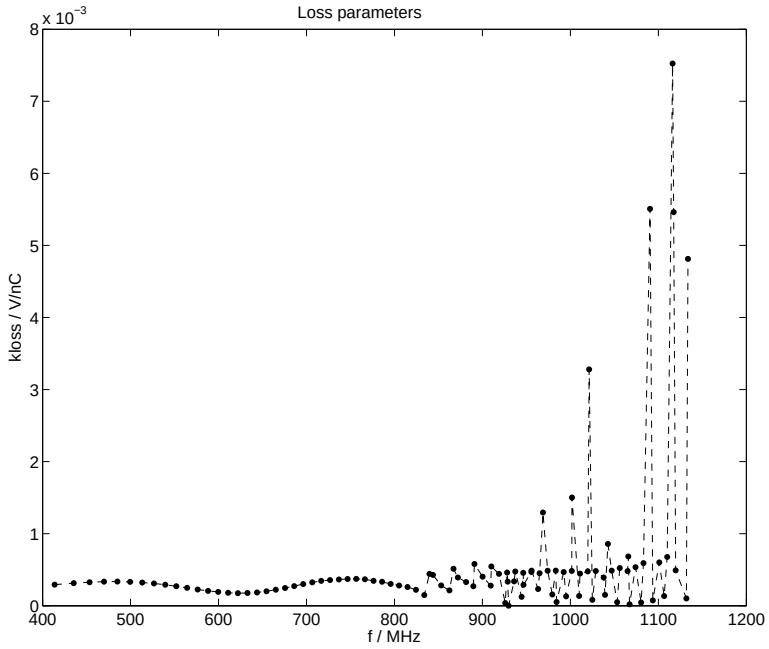

Figure 18: Plot of the loss parameters of the dipole modes at an offset of $r = 1$ cm versus frequency using the data from Tables 13, 14 and 15. The data points are marked (the dotted line is intended only to guide the eye).

The comparison of the loss parameters of the dipole modes calculated for the original geometry (outgoing pipe length of 0.3 m) with two different sets of the boundary conditions (,,electric-electric" and ,,electric-magnetic") at a radius $r = 1$ cm is plotted versus the mode frequency in Fig. 19.

The comparison of the loss parameters of the dipole modes calculated for the original geometry (outgoing pipe length of 0.3 m) and for the geometry with longer (1.3 m) outgoing pipe with ,,electric-electric" boundary conditions at a radius $r = 1$ cm is plotted versus the mode frequency in Fig. 20.

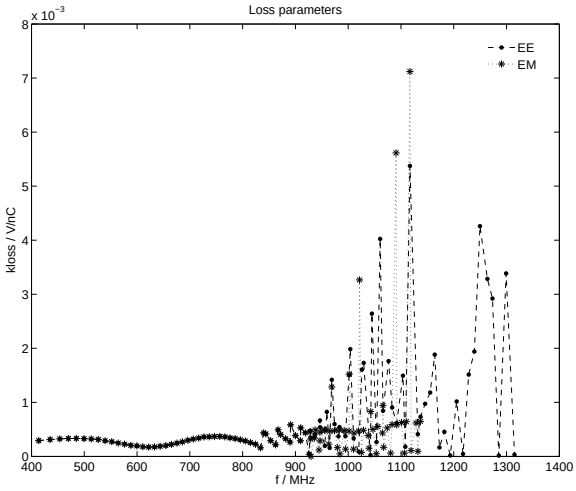

Figure 19: Plot of the loss parameters of the dipole modes at an offset of $r = 1$ cm versus frequency for the original geometry for two sets of boundary conditions („electric-electric" and „electric-magnetic")

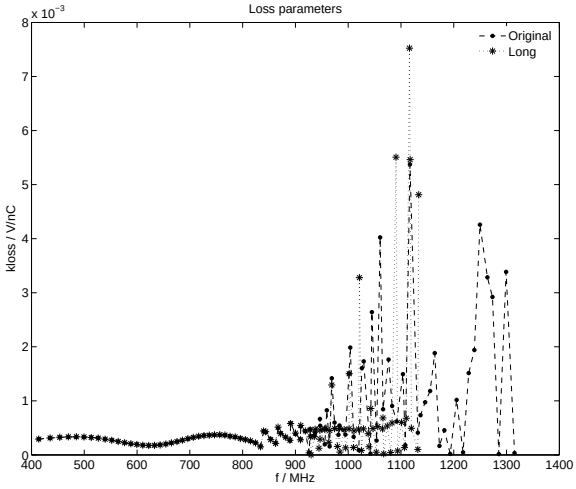

Figure 20: Plot of the loss parameters of the dipole modes at an offset of $r = 1$ cm versus frequency for the original geometry and for the geometry with longer outgoing pipe (1.3 m) with „electric-electric" boundary conditions.

The transverse (dipole) impedance due to HOMs can be obtained as the following sum:

$$Z_\perp(\omega) = \sum_n \frac{Z_{\perp n}}{Q_n} \frac{i\omega_n^2}{\omega^2 - \omega_n^2 + i\omega\omega_n/Q_n}. \tag{21}$$

Parameters for all considered dipole modes from Tables 13, 14, 15 are used in this relation. The real part of the transverse (dipole) impedance is plotted in Fig. 21.

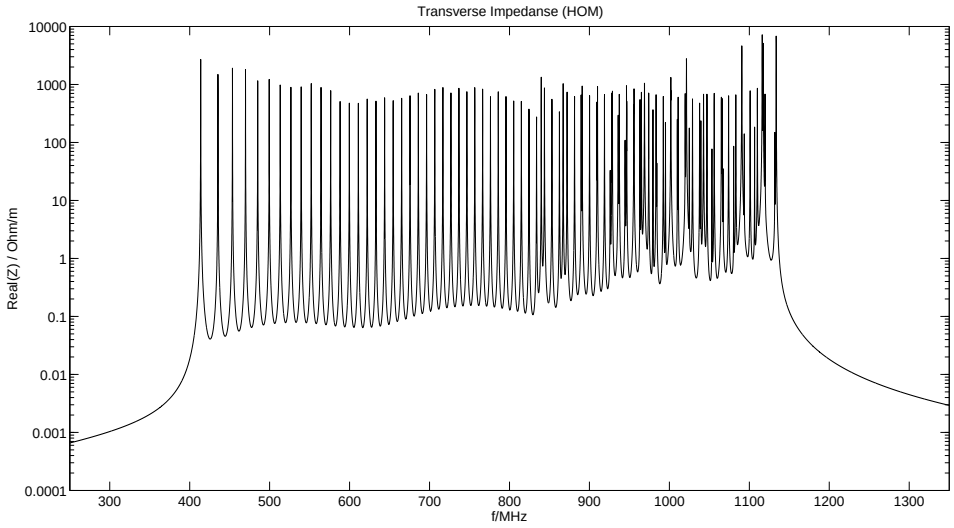

Figure 21: Real part of the transverse (dipole) impedance due to HOMs using the data from Tables 13, 14 and 15

.

4 Summary

The wakefields and higher order modes of the new beam pipe of the ALICE detector for the High Luminosity LHC (HL-LHC) configuration have been calculated with the ECHO2D code [4, 5] and the MAFIA code [9]. The calculations have been done for a 2D model of the vacuum chamber. The radius of the central beam pipe in the region of the IP is 18.2 cm, while elements with maximal radii in the ALICE vacuum chamber are located in two regions: the region of the elliptical beam pipe from 12.5 m to 9 m left from the IP ($r = 95.0$ mm) and the region of the tapering 10 m to 18.5 m right from the IP ($r = 225.0$ mm). Most of the 100 HOMs are trapped in these regions. The maximal loss parameters are $k^{(0)}$=16.45 V/nC for monopole modes, and $k^{(1)}(r)/r^2$=75.24 V/(nCm^2) for dipole modes.

The loss and the kick parameters were obtained also as result of the time domain analysis. The loss parameter of the ALICE vacuum chamber is small (about $2.0\,10^{-2}$ V/pC). The kick parameter of the vacuum chamber without bellows is 4.81 V/pCm. It is larger than the value of the kick parameter for the CMS vacuum chamber (2.38 V/pCm) [2] (for the rms bunch length $\sigma_z = 7.5$ cm), and it is also larger than the value of the kick parameter for the ATLAS vacuum chamber without bellows (1.72 V/pCm) [3] due to the contribution from the step-out transition. The step-out transition between the ingoing (40 mm) and the outgoing (50 mm) pipes of the ALICE structure increases the value of the kick parameter. The kick parameter of the step-out transition is about 2.18 V/pCm. Two bellows increase also the value of the kick parameter of the vacuum chamber. The kick parameter of one bellow is about 2.1 V/pCm. The total kick parameter of the ALICE vacuum chamber with two bellows and the step-out transition can be estimated to be about 8.68 V/pCm.

Acknowledgment

The research leading to these results has received funding from the European Commission under the FP7 project HiLumi LHC, GA no. 284404. We would like to thank Elias Métral for his guidance as task leader of Task 2.4 on impedance issues and collective effects and for valuable discussions. We also thank Benoit Salvant for the timely provision of all details about new design of the ALICE vacuum chamber and for the valuable discussions.

References

[1] O. Brüning, H. Burkhardt, S. Myers, *The Large Hadron Collider*, Progress in Particle and Nuclear Physics, Volume 67, Issue 3, July 2012, Pages 705-734

[2] R. Wanzenberg, O. Zagorodnova, *Calculation of Wakefields and Higher Order Modes for the New Design of the Vacuum Chamber of the CMS Experiment for the HL-LHC*, CERN-ATS-Note-2013-018 TECH, CERN, April 2013

[3] R. Wanzenberg, O. Zagorodnova, *Calculation of Wakefields and Higher Order Modes for the Vacuum Chamber of the ATLAS Experiment for the HL-LHC*, CERN-ACC-Note-2013-0046 TECH, CERN, Nov. 2013

[4] I. Zagorodnov and T. Weiland, *TE/TM field solver for particle beam simulations without numerical Cherenkov radiation*, Phys. Rev. ST Accel. Beams **8** (2005) 042001.

[5] I. Zagorodnov, *Indirect methods for wake potential integration*, Phys. Rev. ST Accel. Beams **9** (2006) 102002 [arXiv:physics/0606049].

[6] T. Weiland, R. Wanzenberg, *Wakefields and Impedances*, in: Joint US-CERN part. acc. school, Hilton Head Island, SC, USA, 7 - 14 Nov 1990, Ed. by M Dienes, M Month and S Turner. - Springer, Berlin, 1992- (Lecture notes in physics ; 400) - pp.39-79.

[7] W.K.H. Panofsky, W.A. Wenzel, *Some consideration concerning the transverse deflection of charged particles in radio-frequency fields* , Rev. Sci. Inst. Vol 27, 11 (1956), 967.

[8] T. F. Günzel, *Transverse Coupling Impedance Of The Storage Ring At The European Synchrotron Radiation Facility*, Phys. Rev. ST Accel. Beams **9** (2006) 114402.

[9] T. Weiland, *On the numerical solution of Maxwell's Equations and Applications in the Field of Accelerator Physics*, Part. Acc. 15 (1984), 245-292.

[10] *MAFIA Release 4 (V4.200)* CST AG, Bad Nauheimer Str. 19, 64289 Darmstadt, Germany.

[11] T. Weiland, *On the computation of resonant modes in cylindrically symmetric cavities*, NIM 216 (1983) 329-348.

[12] D.R. Lide, Ed. *Handbook of Chemistry and Physics* , 79th edition, 1998-1999, CRC Press, Washington, D.C.

[13] P.B. Wilson *High Energy Electron Linacs: Application to Storage Ring RF Systems and Linear Colliders*, AIP Conference Proceedings 87, American Institute of Physics, New York (1982),p. 450-563.